CHEMISTRY
A EUROPEAN JOURNAL

DOI: 10.1002/chem.200701507

Au-Induced Polyvinylpyrrolidone Aggregates with Bound Water for the Highly Shape-Selective Synthesis of Silica Nanostructures

Jianhui Zhang,* Huaiyong Liu, Zhenlin Wang, and Naiben Ming[a]

Abstract: Novel Au-induced polyvinylpyrrolidone (PVP) aggregates with bound water (PVP–water) were created for the highly shape-selective synthesis of distinctive silica nanostructures, such as core–shell spheres, rods, snakes, tubes, capsules, thornlike, and dendritic morphologies. A water/PVP/*n*-pentanol system was first designed to bind water to PVP, and then Au nanoparticles were used to induce the PVP–water species to aggregate into distinctive soft structures by exploiting the interplay between PVP and gold. This was confirmed by the IR absorption spectra. The bound water in the soft structures was consumed during the hydrolysis of tetraethylorthosilicate and the target silica nanostructures were obtained. The soft structures, and therefore, the silica morphologies, can be readily tuned by adjusting the experimental parameters. The tunable Au-induced PVP–water soft structures reported herein open up new dimensions for the synthesis of distinctive nanomaterials (other than silica) that have new physicochemical properties and applications. These soft structures were also successfully extended to synthesize ZnO and SnO_2 particles with remarkable shapes, such as spheres, leaves, T-shaped structures, and dendritic morphologies.

Keywords: biomimetic synthesis · electron microscopy · gold · nanostructures · silica

Introduction

As a result of their broad applications in catalysis, separation, sensor technologies, medical materials, bioprobes, and optics,[1–16] numerous efforts have been devoted to the preparation of distinct silica nanostructures, such as spheres,[4] hollow spheres,[5] tubes,[6] complex core–shell colloids of $Au@SiO_2$[7] and SiO_2@Ag/Cu,[8] nanowires and nanorods,[9] fibers,[10] mesoporous silica,[11] and helical architectures.[12–13] One of the most promising methods in this field is the biomimetic strategy. By using surfactants or polymers as structure-directing agents, biomimetic control of the silica dimensions is achieved,[4c] and also novel or complex silica nanostructures can be created, such as plates,[4e–g,10f,11i] high-aspect-ratio tubules, ribbons with helical architectures,[13] hybrid mesostructures,[11b,f–g,13–15] doughnuts,[11j] and chiral structures.[16]

Herein we report a new Au-assisted biomimetic route that uses polyvinylpyrrolidone (PVP) as a structure-directing agent for the shape-selective synthesis of silica nanostructures. PVP was chosen for the following reasons: First, in high-concentration solutions of PVP in water, the water molecules become bound by PVP to form a PVP–water species, and the water does not act as a solvent in the usual sense. Indeed, it is customary to refer to the water in the PVP–water species as bound water.[17] We have been able to achieve highly shape-selective syntheses of silica by controlling the hydrolysis of tetraethylorthosilicate (TEOS) by using PVP–water. Second, PVP has been extensively used as a stabilizer and structure-directing agent in nanotechnology owing to its excellent adsorption ability.[8,18,19] For example, by using PVP as a stabilizer we managed to prevent agglomeration when coating silica/polystyrene colloids with metals, alloys, and TiO_2,[8,18] and also achieved highly shape-selective syntheses of Au octahedrons and belts; Ag, Au, and Pd nanoprisms; and lamellar ZnO structures by using PVP as a director.[19] Third, PVP is more suitable for biological purposes than previously reported directing agents, such as silaffins, polyamines,[4c–d,5d,10f–i,11p] polypeptides,[4e–g] sodium polymethacrylate,[5c] viruses,[9g] liposomes,[11f] poly(phenylene ethynylene) (PPE),[11g] enzyme aggregates,[11h] cetyltrimethylammonium bromide (CTAB),[11j] lipid molecules,[13] lyotropic liquid-crystalline polymers,[11i,14] block copoly-

[a] Prof. J. Zhang, H. Liu, Prof. Z. Wang, Prof. N. Ming
National Laboratory of Solid State Microstructures
Department of Physics
Nanjing University
Nanjing, 210093 (China)
Fax: (+86) 25-8359-5535
E-mail: zhangjh@nju.edu.cn

mers,[5b,10f,11b–e,k–o,15] and achiral or chiral surfactants,[16] because it is a common, bioclean, biocompatible reagent, and is widely used as an additive in food and pharmaceutical products.

To create the PVP–water species, we designed a water/PVP/*n*-pentanol (WPN) system. In this system, PVP concentrates locally in water because it must remain entirely in the aqueous phase of the water/*n*-pentanol system.[20] Therefore, locally high concentrations of PVP in the aqueous phase occur and PVP–water is obtained. In addition, it is likely that PVP acts as a surfactant and keeps the WPN system stable by binding water because it is unable to form microemulsions or micelles in this solvent system. Finally, the interplay between gold nanoparticles and PVP[19a–c] was exploited to induce PVP–water molecules to aggregate into unique soft structures, thus achieving PVP-directed growth of distinctive silica nanostructures.

Results and Discussion

Highly shape-selective synthesis of silica nanoparticles: In a typical synthesis, a concentrated Au nanoparticle suspension (CANS) was diluted with ethanol and added to a solution of PVP in *n*-pentanol in a conical flask with a stopper and stirred at room temperature for 20 min, then ammonia water (25–28 % NH_3 in water) was added. After stirring for a further 30 min, TEOS was added. The reaction solution was then stirred for 12 h and centrifuged; the product obtained was washed, centrifuged, and ultrasonicated three times with ethanol. Table 1 summarizes the reaction conditions for the structures shown in Figures 1 and 2.

Table 1. Reaction conditions for the syntheses of samples shown in Figures 1 and 2.[a]

Entry	Figure	PVP [g]	*n*-Pentanol [mL]	CANS [mL]	Ethanol [mL]	Ammonia water[b] [mL]
1	1a	0.1	20	0.35	2.0	0.45
2	1b	0.2	20	0.35	2.0	0.45
3	1c, d	0.6	20	0.35	2.0	0.45
4	1e	1.0	20	0.35	2.0	0.45
5	1f	1.0	20	0.30	2.0	0.45
6	1g	1.0	20	0.25	2.0	0.45
7	1h	1.0	20	0.10	2.0	0.45
8	2a	1.0	20	0.35	0.0	0.45
9	2b, c	1.0	20	0.35	0.0	0.55
10	2d, e	1.0	20	0.35	1.0	0.55
11	2f, g	2.0	20	0.65	2.0	0.45
12	2h	2.0	20	0.65	2.0	0.50

[a] TEOS (0.2 mL) was used in each reaction. [b] 25–28 % NH_3 in water.

As seen in Figure 1a (Table 1 entry 1), the product is dominated by Au@silica core–shell spheres with an average diameter of 180 nm. Upon increasing the amount of PVP, sphere growth is suppressed and rods with an average length of 1.0 μm, which have a round head with an average diameter of 0.2 μm and a pointed tip, are formed (Figure 1b; Table 1, entry 2). These rods have an average aspect ratio of

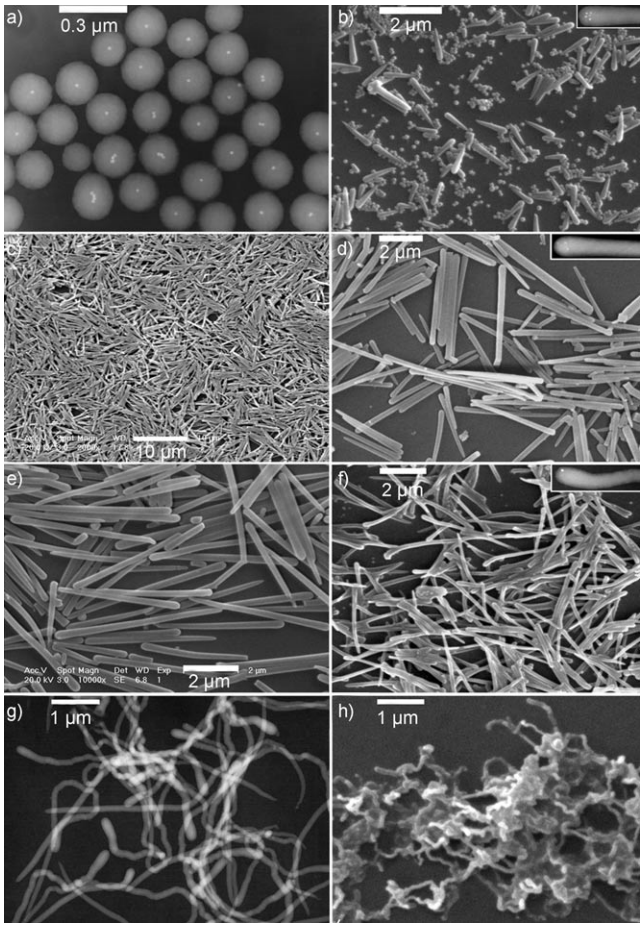

Figure 1. Transition electron microscopy (TEM) and scanning electron microscopy (SEM) images of typical solid silica nanostructures of Au@silica core–shell spheres (a); rods with aspect ratios of 5 (b), 13 (c and d), and 20 (e); slightly bent rods (f); snakelike rods (g); and shapeless fibers (h). Insets of b), d) and f) show the corresponding high-magnification TEM images, in which Au nanoparticles are visible as white spots. Reaction conditions are given in Table 1, entries 1–7.

5 (defined as rod length/head diameter), and gradually decrease in diameter from head to tip. On further increasing the amount of PVP, sphere formation is further suppressed, whereas the yield ratio, size, and aspect ratio of the rods are increased. By using 0.6 g of PVP (Figure 1c and d; Table 1, entry 3), only rods with an average aspect ratio of 13 are obtained (ca. 100 % pure). If the amount of PVP is further increased, the average length (5.5 μm) and aspect ratio (20) of the rods are also increased (Figure 1e; Table 1, entry 4). By keeping the amount of PVP constant and reducing the volume of CANS, the rods can be slightly bent (Figure 1f; Table 1, entry 5) or twisted into snakelike shapes (Figure 1g; Table 1, entry 6). If the CANS volume is significantly reduced, only shapeless fibers are formed (Figure 1h; Table 1, entry 7).

The solid silica rods can be readily changed into hollow silica nanostructures by using CANS in the absence of ethanol. Under the reaction conditions given in Table 1, entry 8, in which CANS is directly added to the reaction so-

lution, the product is dominated by tubes with one or two closed ends. As seen in Figure 2a (Table 1; entry 8), most of the tubes have a uniform outer (ca. 160 nm) and inner diameter (ca. 27 nm) along their lengths. By increasing the volume of ammonia water, both ends of most of the tubes can be opened (Figure 2b), and one of the ends is sharpened into a tip (Figure 2c; Table 1, entry 9). The sharp end and uniform inner wall of this type of nanotube may facilitate the transport of fluids in nanochannels and could also have biochemical applications, such as nanosyringes for cells. In addition, by adjusting the volume of ethanol used to dilute the CANS (Table 1, entry 10), silica capsules (intermediary products between rods and tubes) can be successfully synthesized. As seen in Figure 2d and e, the broken capsules clearly show their hollow nature. We anticipate that these hollow silica capsules could be excellent delivery agents for drugs or catalysts in the near future. In addition, hybrid products of rods and tubes can be prepared by modifying the experimental parameters (Table 1, entry 11) to give thorn-shaped particles (Figure 2f and g). The high-magnification TEM image (Figure 2g) clearly confirms that these thorn-shaped particles are hybrids composed of a tube-shaped trunk and a rodlike branch. Note that the rodlike branch is usually perpendicular to the trunk. The number of rodlike branches is sensitive to the volume of ammonia water in the reaction mixture, and dendritic hybrids composed of one tube-shaped trunk and many rodlike branches can be obtained by increasing the volume of ammonia water (Figure 2h; Table 1, entry 12).

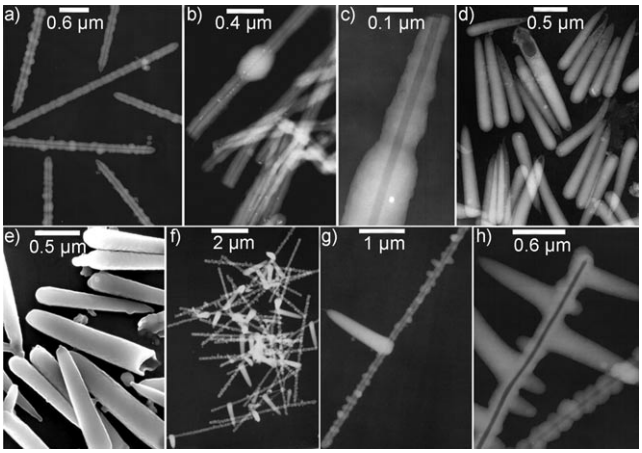

Figure 2. TEM and SEM images of typical hollow silica nanostructures: tubes with closed ends (a), tubes with open ends (b and c), capsules (d and e), hybrid particles (composed of tube-shaped trunks and rodlike branches) with thornlike (f and g) and dendritic (h) shapes. Au nanoparticles are visible as white spots. Reaction conditions are given in Table 1, entries 8–12.

Growth mechanism of silica nanostructures: To find the key parameters that determine the silica shape, the influences of the quantities of CANS, PVP, and ammonia water and the presence or absence of ethanol have been investigated in detail, and six general rules have been proposed.

1) CANS is the precondition for the formation of anisotropic nanostructures, such as rods, tubes, and capsules. In the core–shell spheres, rods, and tubes (Figures 1 and 2), the Au nanoparticles are generally located at the center of the spheres, the centers of the rodlike heads, and on the walls of the tube, which implies that the initial hydrolysis of TEOS occurs on the surface of the Au nanoparticles. If CANS is replaced by distilled water, only spheres are obtained (Figure 3), irrespective of changes to other experimental parameters. Furthermore, the hydrolysis reaction becomes very slow. The formation of these spheres should be related to a modified Stöber process.[4a,h]
2) The use of ethanol to dilute the CANS can accelerate the hydrolysis reaction and facilitate rod formation, but also suppresses tube growth. This is consistent with the fact that ethanol facilitates the hydrolysis of TEOS.[21] Hollow capsules, the intermediary products between rods and tubes, can be prepared by rationally modifying the volume of ethanol in the reaction mixture.
3) A small amount of PVP ($\leq$0.1 g) and/or a large total water volume ($\geq$1.3 mL) and/or a high volume ratio of ammonia water to total water (VRAW, $\geq$0.75) leads to an overly quick hydrolysis reaction, and only silica spheres are obtained.
4) An increase in the amount of PVP can change the main product shape from spheres to anisotropic structures, such as rods, tubes (Figure 4a), and capsules. The specific anisotropic structures obtained are dependent on the volume of ethanol used to dilute the CANS.
5) A reduction in the volume of water and changes to the VRAW have similar effects on the silica shape as an increase in the amount of PVP. However, when the total water volume is reduced to 0.75 mL or the VRAW is 0.3 or lower, the hydrolysis of TEOS is greatly suppressed and the final product tends to be bent (see Figures 1f and 4b) or twisted (see Figure 1g and h).
6) By simultaneously using a large volume of water (1.0–1.2 mL) and more than 1.5 g of PVP, the formation of hybrids of rods and tubes is facilitated (see Figure 2f–h).

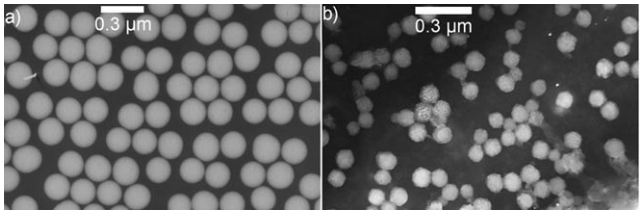

Figure 3. TEM images of typical silica spheres synthesized under different conditions in the absence of Au nanoparticles. Reaction conditions: a) distilled water (0.4 mL), ammonia water (0.6 mL), PVP (0.2 g); b) distilled water (0.35 mL), ammonia water (0.45 mL), PVP (1.0 g).

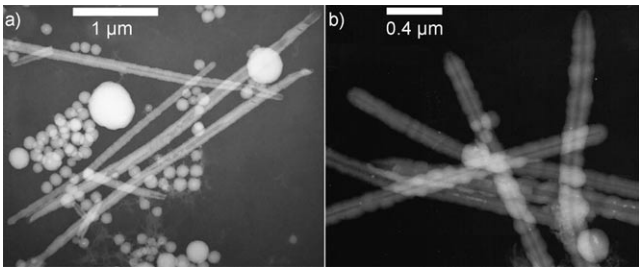

Figure 4. TEM images of typical silica tubes synthesized under different conditions. Reaction conditions: a) CANS (0.35 mL), ammonia water (0.45 mL), PVP (0.4 g); b) CANS (0.25 mL), ammonia water (0.45 mL), PVP (1.0 g).

To further understand the roles of PVP and Au, the dispersed Au nanoparticles were obtained by centrifugation from solutions that contained the mixtures shown Table 1, entries 4 and 8, before TEOS was added. These samples were labeled Au1 (Table 1, entry 8) and Au2 (Table 1, entry 4), and were dispersed on silicon substrates for characterization by IR spectroscopy. For comparison, the IR spectra of as-prepared Au nanoparticles and pure PVP were also recorded (Figure 5). PVP has some typical bond absorptions around $\tilde{\nu}=1284$, 1427, 1666, 2925, and 3433 cm^{-1}, which arise from the absorptions of N→H–O, the pyrollidone ring, and the bond vibrations of C=O, C–H, and O–H (from water impurities), respectively.[20] In contrast with the as-prepared Au nanoparticles, both Au1 and Au2 also show several typical absorption bands related to PVP. Compared to pure PVP, the C–H band in Au1 remains in the same position because the hydrocarbon chain is inert to Au. However, the bands that arise from N→H–O, the pyrollidone ring, C=O, and O–H are slightly redshifted to $\tilde{\nu}=1273$, 1412, 1641, and 3425 cm^{-1}, respectively. In Au2, the bands that arise from N→H–O, the pyrollidone ring, and O–H are further redshifted to 1245, 1405, and 3403 cm^{-1}, respectively, and the C=O band is separated into two bands at 1636 and 1719 cm^{-1}. These redshifts can be attributed to bond weakening that arises from the partial donation of the O/N lone-pair electrons of PVP to vacant orbitals on the Au surface.

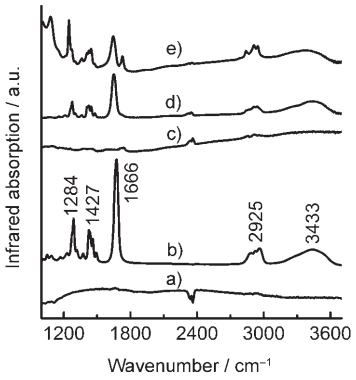

Figure 5. IR absorption spectra of a) the silicon substrate, b) pure PVP, c) as-prepared Au nanoparticles, d) Au1 nanoparticles, and e) Au2 nanoparticles.

In particular, this relates to the coordination bonds formed between O/N atoms and specific Au crystallographic planes. Therefore, the coagulation of PVP on Au does indeed occur as a result of the interplay between PVP and Au. Furthermore, the coordination bonds between PVP and Au weaken the O–H bond, which weakens the interaction between PVP and water and facilitates the hydrolysis of TEOS on PVP. The interaction between PVP and water can be further weakened by diluting the CANS with ethanol. PVP can also be partly dissolved by ethanol, which reduces the PVP concentration in water to further weaken the PVP–water interaction.[20]

To monitor the silica growth process, time-dependent TEM images of the products formed during the synthesis of the snakelike nanoparticles (Figure 1g; Table 1, entry 6) were recorded. After a reaction time of 3 h, the product was dominated by semitransparent snakelike rods (Figure 6a),

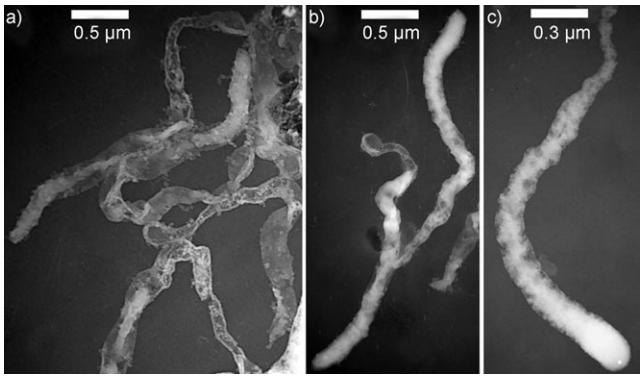

Figure 6. TEM images of products formed after a) 3, b) 6, and c) 9 h. Reaction conditions: PVP (1.0 g) in *n*-pentanol (20 mL), CANS (0.25 mL) in ethanol (2 mL), and ammonia water (0.45 mL).

which could freely twist and bend. In some of the rods, silica had preferentially formed and deposited at the center and head of the rod. Silica was continuously deposited in the rods as the reaction progressed, and after 6 h the rods were mostly filled, except for the tail (Figure 6b). After 9 h, almost the entire rods were filled with silica, and snakelike silica rods with rough surfaces were obtained (Figure 6c). After 12 h, silica completely filled the rods, and snakelike silica rods with a smooth surface were obtained (Figure 1g). These results clearly indicate that our method involves a soft template growth process.

Based on the results and discussions above, three silica growth models are proposed. 1) After CANS is added, Au nanoparticles coordinate with PVP–water molecules and induce the aggregation of PVP into soft structures. When a small amount of PVP and/or a large VRAW is used, the soft structure adopts a spherical shape (Figure 7a). This structure allows a small amount of PVP to maximize the amount of PVP–water formed and minimize the interface area between the soft structure and *n*-pentanol, which helps to stabilize the WPN system. After the bound water in the spherical soft structure has been consumed by the hydrolysis of

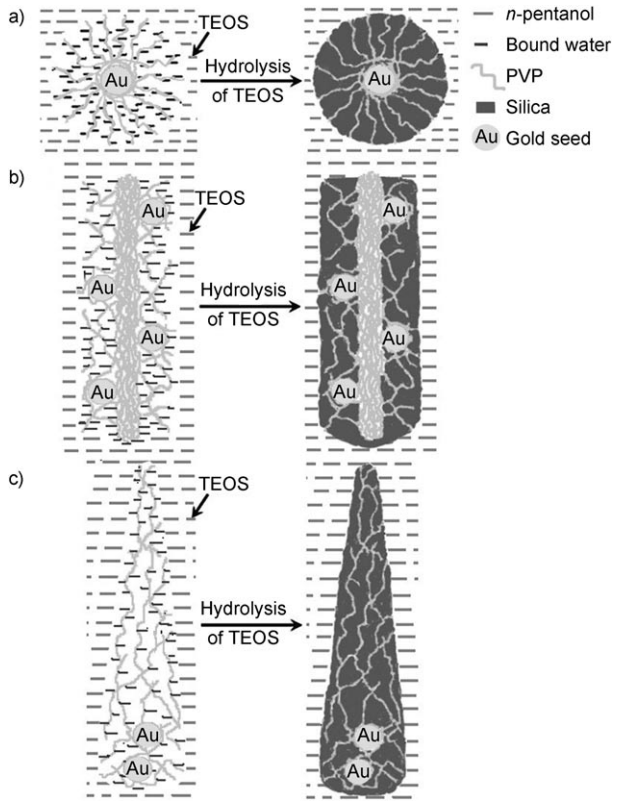

Figure 7. Proposed growth models for a) silica spheres, b) tubes, and c) rods.

TEOS, an Au@silica core–shell sphere is formed. 2) If the amount of PVP is increased, the excess PVP molecules are less likely to bind water and more likely to aggregate into a dendritic form (composed of a compact trunk with no bound water and loose branches with bound water; Figure 7b) to reduce the energy of the system. After the bound water in the branches is consumed by the hydrolysis of TEOS, a tubelike structure is observed because PVP is transparent under the TEM electron beam or the trunk is dissolved by ethanol during the washing process. If the ends of the trunk are capped with bound water, the tube ends will be closed; conversely, if the trunk is not capped with bound water, the tube ends will be open. 3) By using a large amount of PVP and simultaneously diluting the CANS with ethanol, the solubility of PVP is increased and the formation of a compact trunk is suppressed. PVP tends to coagulate into the rod form (Figure 7c). After the bound water is consumed by the hydrolysis of TEOS, a silica rod is formed.

By carefully controlling the amounts of PVP, CANS, ammonia water, and ethanol, soft structures with a tip, hybrid soft structures, and bent soft structures can be achieved. After the addition and hydrolysis of TEOS, these structures result in the formation of capsules (Figure 2d and e), T-shaped (Figure 2f–g), and bent rod and tube (Figure 1g and 4b) structures, respectively. We believe that these silica structures reflect the specific structures of the PVP aggregates in our WPN system.

Highly shape-selective synthesis of ZnO and SnO_2 particles: As demonstrated above, our route uses Au nanoparticles as the precondition for the formation of PVP–water soft structures, and thereby the target silica anisotropic nanostructures. This conclusion has been further confirmed by extending our method to the preparation of ZnO and SnO_2 particles with controlled shapes. In a typical synthesis of ZnO particles, an aqueous solution of NaOH (0.7 mL, 0.0714 M) was added to solution of PVP (0.07 g) in *n*-pentanol (20 mL) with stirring. After 30 min, a solution of $Zn(NO_3)_2{\cdot}6H_2O$ (0.08 M) in ethanol (0.8 mL) was added and the mixture was stirred for another 30 min. The mixture was then heated at 95 °C in a constant-temperature oven for two days. As shown in Figure 8a, the product obtained was dominated by monodisperse amorphous spheres with a diameter of 210 nm. If the aqueous NaOH was replaced by a mixture of CANS (0.3 mL) and aqueous NaOH (0.4 mL, 0.125 M), and the NaOH concentration and water volume were kept constant, irregular lamellar particles (Figure 8b) were obtained, which showed that the anisotropic growth of ZnO was induced by the addition of Au nanoparticles. If the amount of PVP is increased to 1.0 g, only leaflike particles are obtained (Figure 8c). The corresponding selected-area electron diffraction (SAED) pattern (Figure 8, inset; obtained from a single particle lying flat on a support film with the electron beam perpendicular to the leaflike facets) clearly shows the single-crystalline nature of these leaflike particles. A further increase in the amount of PVP to 1.4 g leads to the formation of T-shaped particles (Figure 8d) that are similar to the thornlike silica particles.

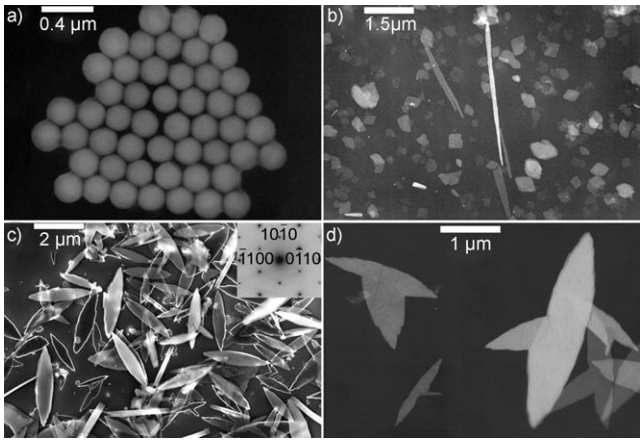

Figure 8. TEM and SEM images of ZnO particles with controlled shapes: a) spheres, b) irregular lamellar particles, c) leaflike particles, and d) T-shaped particles. The inset of c) shows the corresponding selected-area electron diffraction (SAED) pattern.

The synthesis of SnO_2 particles is similar to that of ZnO particles, except that the solution of $Zn(NO_3)_2{\cdot}6H_2O$ in ethanol is replaced by $SnCl_4{\cdot}5H_2O$ in ethanol. By using aqueous NaOH (0.7 mL, 0.4 M), a solution of $SnCl_4{\cdot}5H_2O$ (0.1 M) in ethanol (0.8 mL), and PVP (0.07 g), monodisperse amorphous spheres are obtained (Figure 9a). If aqueous

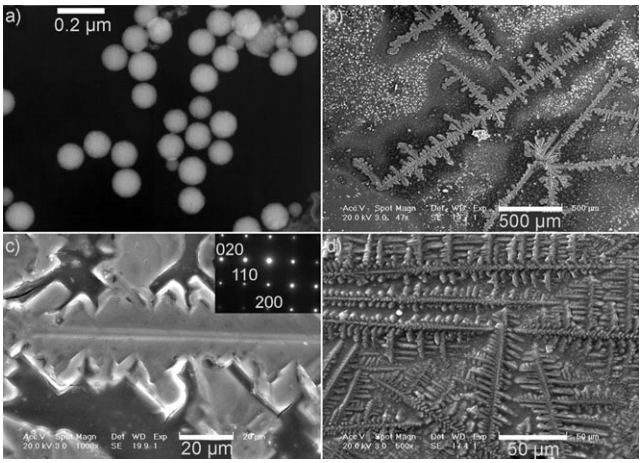

Figure 9. TEM and SEM images of SnO_2 particles with controlled shapes: a) spheres, b) impure dendritic particles, c) a highly magnified image of a dendritic particle, and d) pure dendritic particles. The inset of c) shows the corresponding SAED pattern.

NaOH is replaced by a mixture of CANS (0.3 mL) and aqueous NaOH (0.4 mL, 0.7 M), dendritic particles that resemble the shapes of dendritic silica particles are formed (Figure 9b and c). The SAED pattern (Figure 9c, inset) shows the single-crystalline nature of these dendritic particles. The purity of the dendritic particles can be greatly improved by increasing the amount of PVP to 1.0 g (Figure 9d). This Au-induced growth of anisotropic ZnO and SnO_2 particles not only further confirms the crucial role of Au, but also suggests that the Au-induced PVP–water aggregates demonstrated herein could give new insights into the highly shape-selective synthesis of anisotropic functional nanoparticles.

Conclusion

In summary, a novel biomimetic method has been developed for the highly shape-selective synthesis of silica nanostructures. Four important results are highlighted in this work: 1) As a result of the interplay between PVP, water, and Au, Au-induced PVP–water soft structures have been successfully created, which confine the hydrolysis of TEOS along the PVP surface for the first time. The soft structures, and thus, the final silica morphologies, can be easily modified by adjusting the amounts of PVP, CANS, and ammonia water, and by using ethanol to dilute the CANS. 2) Up to ten kinds of highly pure distinctive or novel silica nanostructures, such as capsules and thornlike nanostructures, have been produced on a large scale. Furthermore, the product size and/or aspect ratio can be tuned across a large range. Typically, silica rods with lengths of 0.18 to 5.5 μm and aspect ratios of 1 to 20 were obtained, whereas only one, or a few, types of shapes within a narrow size range can be prepared by most of the previously reported biomimetic methods.[4c–h,5c–d,9g,10f–i,11–16] We believe that it will be possible to synthesize other novel silica nanostructures with high purity and controllable sizes by optimizing the experimental parameters of our method. 3) The analysis of the IR absorption spectra verifies the interplay between PVP, water, and Au, and confirms that the addition of ethanol and the interplay between PVP and Au can weaken the strength of the interaction between PVP and water and facilitate the hydrolysis of TEOS. 4) The tunable Au-induced PVP–water soft structures created herein can provide a new, versatile route for the shape-selective synthesis of nanomaterials other than silica, and has been successfully exploited to prepare ZnO and SnO_2 particles with distinctive shapes, such as spheres, leaves, T-shaped structures, and dendritic morphologies, on a large scale.

Experimental Section

$HAuCl_4 \cdot H_2O$ (analytical reagent, AR, $\geq$99.95%), PVP (average molecular weight $M_n = 30000$), $C_6H_5O_7Na_3 \cdot 2H_2O$ (AR, $\geq$99.0%), TEOS (AR, SiO_2 = 27.9%), ammonia water (AR, 25–28% NH_3), *n*-pentanol (AR, $\geq$99.0%), and ethanol (AR, $\geq$99.7%) were used as received. The sample morphology was examined by using SEM (XL30, Phillips, The Netherlands) and TEM (JEM-200CX, JEOL, Japan). The IR absorption spectra of samples dispersed on silicon substrates were collected by using a far-field Fourier transform infrared spectrometer (Nicolet 5700, USA).

Synthesis of Au nanoparticles (ca. 10 nm): Aqueous $HAuCl_4 \cdot 4H_2O$ (3 mL, 0.03 M) and aqueous $C_6H_5O_7Na_3 \cdot 2H_2O$ (6 mL, 0.034 M) were sequentially added to boiling water (360 mL). After boiling for 15 min, the as-prepared suspension was obtained and then it was concentrated to ten times its original concentration upon standing.

Acknowledgements

The work was supported by the NSFC (project 10404013) and by a grant from the State Key Program for Basic Research of China. P. Zhan and X. N. Zhao are gratefully acknowledged for their assistance with SEM measurements.

[1] N. K. Raman, M. T. Anderson, C. J. Brinker, *Chem. Mater.* **1996**, *8*, 1682–1701.
[2] A. Sayari, *Chem. Mater.* **1996**, *8*, 1840–1852.
[3] X. Feng, G. E. Fryxell, L.-Q. Wang, A. Y. Kim, J. Liu, K. M. Kemner, *Science* **1997**, *276*, 923–926.
[4] a) J. H. Zhang, P. Zhan, Z. L. Wang, W. Y. Zhang, N. B. Ming, *J. Mater. Res.* **2003**, *18*, 649–653; b) T. Yanagishita, Y. Tomabechi, K. Nishio, H. Masuda, *Langmuir*, **2004**, *20*, 554–555; c) M. Sumper, S. Lorenz, E. Brunner, *Angew. Chem.* **2003**, *115*, 5350–5353; *Angew. Chem. Int. Ed.* **2003**, *42*, 5192–5195; d) J.-J. Yuan, R.-H. Jin, *Adv. Mater.* **2005**, *17*, 885–888; e) M. M. Tomczak, D. D. Glawe, L. F. Drummy, C. G. Lawrence, M. O. Stone, C. C. Perry, D. J. Pochan, T. J. Deming, R. R. Naik, *J. Am. Chem. Soc.* **2005**, *127*, 12577–12582; f) D. D. Glawe, F. Rodríguez, M. O. Stone, R. R. Naik, *Langmuir* **2005**, *21*, 717–720; g) F. Rodríguez, D. D. Glawe, R. R. Naik, K. P. Hallinan, M. O. Stone, *Biomacromolecules*, **2004**, *5*, 261–265; h) W. Stöber, A. Fink, E. Bohn, *J. Colloid Interface Sci.* **1968**, *26*, 62–69.
[5] a) F. Caruso, R. A. Caruso, H. Möhwald, *Science* **1998**, *282*, 1111–1114; b) A. Khanal, Y. Inoue, M. Yada, K. Nakashima, *J. Am. Chem. Soc.* **2007**, *129*, 1534–1535; c) M. Fujiwara, K. Shiokawa, I. Sakakura, Y. Nakahara, *Nano Lett.* **2006**, *6*, 2925–2928; d) C. A. Bauer, D. B. Robinson, B. A. Simmons, *Small* **2007**, *3*, 58–62.

[6] a) B. Yao, D. Fleming, M. A. Morris, S. E. Lawrence, *Chem. Mater.* **2004**, *16*, 4851–4855; b) K. J. C. van Bommel, J. H. Jung, S. Shinkai, *Adv. Mater.* **2001**, *13*, 1472–1476.
[7] S. Liu, M. Han, *Adv. Funct. Mater.* **2005**, *15*, 961–967.
[8] a) J. Zhang, J. Liu, S. Wang, P. Zhan, Z. Wang, N. Ming, *Adv. Funct. Mater.* **2004**, *14*, 1089–1096; b) J. Zhang, H. Liu, Z. Wang, N. Ming, *J. Solid State Chem.* **2007**, *180*, 1291–1297.
[9] a) C. Yu, J. Fan, B. Tian, D. Zhao, G. D. Stucky, *Adv. Mater.* **2002**, *14*, 1742–1745; b) Z. Yang, Z. Niu, X. Cao, Z. Yang, Y. Lu, Z. Hu, C. C. Han, *Angew. Chem.* **2003**, *115*, 4333–4335; *Angew. Chem. Int. Ed.* **2003**, *42*, 4201–4203; c) S. Giri, B. G. Trewyn, M. P. Stellmaker, V. S.-Y. Lin, *Angew. Chem.* **2005**, *117*, 5166–5172; *Angew. Chem. Int. Ed.* **2005**, *44*, 5038–5044; d) S. J. Limmer, G. Cao, *Adv. Mater.* **2003**, *15*, 427–431; e) D. P. Yu, R. L. Hang, Y. Ding, H. Z. Zhang, Z. G. Bai, J. J. Wang, Y. H. Zou, W. Qian, G. C. Xiong, S. Q. Feng, *Appl. Phys. Lett.* **1998**, *73*, 3076–3078; f) A. Sayari, B.-H. Han, Y. Yang, *J. Am. Chem. Soc.* **2004**, *126*, 14348; g) Z. Zhang, J. Buitenhuis, *Small* **2007**, *3*, 424–428.
[10] a) S. Schacht, Q. Huo, I. G. Voigt-Martin, G. D. Stucky, F. Schüth, *Science* **1996**, *273*, 768–771; b) P. J. Bruinsma, A. Y. Kim, J. Liu, S. Baskaran, *Chem. Mater.* **1997**, *9*, 2507–2512; c) F. Kleitz, F. Marlow, G. D. Stucky, F. Schüth, *Chem. Mater.* **2001**, *13*, 3587–3595; d) F. Marlow, M. D. McGehee, D. Zhao, B. F. Chmelka, G. D. Stucky, *Adv. Mater.* **1999**, *11*, 632–636; e) J. Wang, J. Zhang, B. Y. Asoo, G. D. Stucky, *J. Am. Chem. Soc.* **2003**, *125*, 13966–13967; f) P.-X. Zhu, N. Fukazawa, R.-H. Jin, *Small* **2007**, *3*, 394–398; g) J.-J. Yuan, P.-X. Zhu, N. Fukazawa, R.-H. Jin, *Adv. Funct. Mater.* **2006**, *16*, 2205–2212; h) R.-H. Jin, J.-J. Yan, *Macromol. Chem. Phys.* **2005**, *206*, 2160–2170; i) R.-H. Jin, J.-J. Yan, *Chem. Mater.* **2006**, *18*, 3390–3396.
[11] a) H. Yang, N. Coombs, G. A. Ozin, *Nature* **1997**, *386*, 692–695; b) H. Song, R. M. Rioux, J. D. Hoefelmeyer, R. Komor, K. Niesz, M. Grass, P. Yang, G. A. Somorjai, *J. Am. Chem. Soc.* **2006**, *128*, 3027–3037; c) K. Flodström, V. Alfredsson, N. Källrot, *J. Am. Chem. Soc.* **2003**, *125*, 4402–4403; d) K. Suzuki, K. Ikari, H. Imai, *J. Am. Chem. Soc.* **2004**, *126*, 462–463; e) T.-W. Kim, F. Kleitz, B. Paul, R. Ryoo, *J. Am. Chem. Soc.* **2005**, *127*, 7601–7610; f) Y. Li, W. T. Yip, *J. Am. Chem. Soc.* **2005**, *127*, 12756–12757; g) A. P.-Z. Clark, K.-F. Shen, Y. F. Rubin, S. H. Tolbert, *Nano Lett.* **2005**, *5*, 1647–1652; h) J. Lee, J. Kim, J. Kim, H. Jia, M. I. Kim, J. H. Kwak, S. Jin, A. Dohnalkova, H. G. Park, H. N. Chang, P. Wang, J. W. Grate, T. Hyeon, *Small* **2005**, *1*, 744–753; i) P. Feng, X. Bu, G. D. Stucky, D. J. Pine, *J. Am. Chem. Soc.* **2000**, *122*, 994–995; j) D. Zhao, J. Sun, Q. Li, G. D. Stucky, *Chem. Mater.* **2000**, *12*, 275–279; k) J. M. Kim, Y. Sakamoto, Y. K. Hwang, Y.-U. Kwon, O. Terasaki, S.-E. Park, G. D. Stucky, *J. Phys. Chem. B* **2002**, *106*, 2552–2558; l) P. Yang, D. Zhao, B. F. Chmelka, G. D. Stucky, *Chem. Mater.* **1998**, *10*, 2033–2036; m) C. Yu, J. Fan, B. Tian, G. D. Stucky, D. Zhao, *J. Phys. Chem. B* **2003**, *107*, 13368–13375; n) D. Zhao, Q. Huo, J. Feng, B. F. Chmelka, G. D. Stucky, *J. Am. Chem. Soc.* **1998**, *120*, 6024–6036; o) D. Zhao, P. Yang, N. Melosh, J. Feng, B. F. Chmelka, G. D. Stucky, *Adv. Mater.* **1998**, *10*, 1380–1385; p) J. Wang, C.-K. Tsung, W. Hong, Y. Wu, J. Tang, G. D. Stucky, *Chem. Mater.* **2004**, *16*, 5169–5181.
[12] S. M. Yang, I. Sokolov, N. Coombs, C. T. Kresge, G. A. Ozin, *Adv. Mater.* **1999**, *11*, 1427–1431.
[13] A. M. Seddon, H. M. Patel, S. L. Burkett, S. Mann, *Angew. Chem.* **2002**, *114*, 3114–3117; *Angew. Chem. Int. Ed.* **2002**, *41*, 2988–2991.
[14] C. G. Göltner, S. Henke, M. C. Weissengerger, M. Antonietti, *Angew. Chem.* **1998**, *110*, 633–636; *Angew. Chem. Int. Ed.* **1998**, *37*, 613–616.
[15] J. Fan, C. Ye, F. Gao, J. Lei, B. Tian, L. Wang, Q. Luo, B. Tu, W. Zhou, D. Zhao, *Angew. Chem.* **2003**, *115*, 3254–3258; *Angew. Chem. Int. Ed.* **2003**, *42*, 3146–3150.
[16] a) B. Wang, C. Chi, W. Shan, Y. Zhang, N. Ren, W. Yang, Y. Tang, *Angew. Chem.* **2006**, *118*, 2142–2144; *Angew. Chem. Int. Ed.* **2006**, *45*, 2088–2090; b) H. Jin, Z. Liu, T. Ohsuna, O. Terasaki, Y. Inoue, K. Sakamoto, T. Nakanishi, K. Ariga, S. Che, *Adv. Mater.* **2006**, *18*, 593–596.
[17] a) A. P. MacKenzie, D. H. Rasmussen in *Water Structure at the Water–Polymer Interface* (Ed.: H. H. G. Jellinek), John Wiley, New York, **1972**; b) M. J. A. de Dood, J. Kalkman, C. Strohhöfer, J. Michielsen, J. van der Elsken, *J. Phys. Chem. B* **2003**, *107*, 5906–5913.
[18] a) J. H. Zhang, S. Z. Wang, J. B. Liu, Z. L. Wang, N. B. Ming, *J. Mater. Res.* **2005**, *20*, 965–970; b) J. Zhang, P. Zhan, H. Liu, Z. Wang, N. Ming, *Mater. Lett.* **2006**, *60*, 280–283.
[19] a) J. Zhang, H. Liu, Z. Wang, N. Ming, *Appl. Phys. Lett.* **2007**, *90*, 163122–163124; b) J. Zhang, H. Liu, P. Zhan, Z. Wang, N. Ming, *Adv. Funct. Mater.* **2007**, *17*, 3295–3303; c) J. Zhang, H. Liu, P. Zhan, Z. Wang, N. Ming, *Appl. Phys. Lett.* **2007**, *91*, 133112–133114; d) J. Zhang, H. Liu, P. Zhan, Z. Wang, N. Ming, *Adv. Funct. Mater.* **2007**, *17*, 1558–1566; e) J. Zhang, H. Liu, P. Zhan, Z. Wang, N. Ming, *Adv. Funct. Mater.* **2007**, *17*, 3897–3905; f) J. Zhang, H. Liu, Z. Wang, N. Ming, *Appl. Phys. Lett.* **2007**, *90*, 113117–113119.
[20] Y. D. Cui, G. B. Yi, L. W. Liao in *The Synthesis and Applications of Polyvinylpyrrolidone*, Science Publishing Company, Beijing, **2001**, pp. 14–24.
[21] R. R. Hao, X. Y. Fang, S. C. Niu in *Inorganic Chemistry Series, Vol. 3: C, Si, and Ge Secondary Groups.* (Ed.: H. Q. Hu), Science Publishing Company, Beijing, **1998**, p. 228.

Received: September 22, 2007
Published online: March 25, 2008

